Border collision route to quasiperiodicity: Numerical investigation and experimental confirmation

Zhanybai T. Zhusubaliyev[a)]
Kursk State Technical University, Department of Computer Science 50 Years of October Street, 94, Kursk 305040, Russia

Erik Mosekilde[b)]
Complex Systems Group, Department of Physics, Technical University of Denmark, 2800 Lyngby, Denmark

Somnath Maity, Srijith Mohanan, and Soumitro Banerjee[c)]
Department of Electrical Engineering, Indian Institute of Technology, Kharagpur-721302, India

(Received 16 September 2005; accepted 4 May 2006; published online 2 June 2006)

Numerical studies of higher-dimensional piecewise-smooth systems have recently shown how a torus can arise from a periodic cycle through a special type of border-collision bifurcation. The present article investigates this new route to quasiperiodicity in the two-dimensional piecewise-linear normal form map. We have obtained the chart of the dynamical modes for this map and showed that border-collision bifurcations can lead to the birth of a stable closed invariant curve associated with quasiperiodic or periodic dynamics. In the parameter regions leading to the existence of an invariant closed curve, there may be transitions between an ergodic torus and a resonance torus, but the mechanism of creation for the resonance tongues is distinctly different from that observed in smooth maps. The transition from a stable focus point to a resonance torus may lead directly to a new focus of higher periodicity, e.g., a period-5 focus. This article also contains a discussion of torus destruction via a homoclinic bifurcation in the piecewise-linear normal map. Using a dc–dc converter with two-level control as an example, we report the first experimental verification of the direct transition to quasiperiodicity through a border-collision bifurcation.
 [DOI: 10.1063/1.2208565]

Application of nonlinear dynamics and chaos theory in practice, particularly in engineering, often leads to the analysis of piecewise-smooth systems. Low-dimensional models of such systems have shown that they can exhibit behavioral transitions, referred to as border-collision bifurcations, that are qualitatively different from the bifurcations we know for smooth dynamical systems. In particular, these bifurcations can produce direct transitions from periodicity to chaos or, for instance, from period-2 to period-3 dynamics. The purpose of this article is to show that torus birth bifurcations (transitions to quasiperiodicity) can also occur via border-collision bifurcations. In this case a pair of complex conjugate Floquet multipliers jump from the inside to the outside of the unit circle. We also examine the border-collision bifurcations through which the ergodic torus is transformed into a resonance torus. Torus destruction represents one of the most complicated routes to chaos, and the possible mechanisms for torus destruction in nonsmooth systems have not yet been examined in detail. A second purpose of the present article is to initiate this analysis. Finally, we illustrate our results through a practical example from power electronics and present the first experimental verification of torus birth via a border-collision bifurcation.

I. INTRODUCTION

Quasiperiodicity is a specific type of dynamic behavior characterized by the coexistence of two (or more) oscillatory modes with incommensurable frequencies. The transition from regular periodic dynamics to quasiperiodicity is most instructively discussed in terms of the Poincaré map, and it is known that this transition in smooth (i.e., everywhere differentiable) maps occur through a Neimark–Sacker bifurcation[1] in which a pair of complex conjugate eigenvalues (Floquet multipliers) for the fixed point cross out of the unit circle in a continuous manner.

However, many systems of practical importance give rise to maps that are not everywhere differentiable. Piecewise-smooth maps typically arise as discrete-time models of dynamical systems where the continuous evolution in time is punctuated by discrete impacts or switching events that alter the form of the constitutive equations. Examples of such systems include switching circuits,[2–7] impact oscillators,[8–10] and walking robots,[11,12] as well as physiological models[13] and various micro- and macroeconomic systems.[14] As a parameter is varied, the fixed point for the Poincaré map of such a system may move in phase space and collide with the borderline between two smooth regions.

[a)]Electronic mail: zhanybai@mail.kursk.ru
[b)]Electronic mail: Erik.Mosekilde@fysik.dtu.dk
[c)]Electronic mail: soumitro@ee.iitkgp.ernet.in

When this happens, the eigenvalues can change abruptly, leading to a special class of nonlinear dynamic phenomena known as border-collision bifurcations.[15–22]

Feigin was presumably first to consider these phenomena in detail. His analyses of mechanical impact oscillators date back to the 1970s.[15–17] In Feigin's work border-collision bifurcations are called C-bifurcations, "C" standing for the Russian word for "sewing." This refers to the fact that one has to "sew" the solutions together across the borderline between two smooth regions. Some of the main results of Feigin's work have subsequently been recast into the framework of modern bifurcation theory by di Bernardo *et al.*[22]

In the western literature, early work on border-collision bifurcations was published by Nusse and Yorke,[19–21] and the term "border-collision bifurcation" was introduced by these authors. Among other phenomena, Nusse and Yorke emphasized the possibility of observing peculiar bifurcations such as direct transitions from period-2 to period-3 dynamics or from regular periodic motion into chaos. Banerjee *et al.*[23–25] developed the theory of border-collision bifurcations in one- and two-dimensional piecewise smooth maps, and illustrated its application in power electronic systems. It was shown that the so-called corner-collision, sliding and grazing bifurcations all belong to this class.[9,26–32] To investigate the various types of bifurcation, a normal form map may be constructed (see, e.g., Refs. 26–29). Recent reviews on border-collision bifurcations in piecewise-smooth mechanical and power electronic systems have been published by Banerjee and Verghese,[33] Blazejczyk-Okolewska *et al.*,[34] Leine and Nijmeijer,[35] Tse,[36] and Zhusubaliyev and Mosekilde.[37]

Evidence from the study of a large number of physical systems,[35,37–43] e.g., switching circuits, impact oscillators, accumulated over the years demonstrates that quasiperiodic dynamics regularly occurs in such systems. The onset of quasiperiodic behavior has been reported in impact oscillators by Piiroinen *et al.*[43] This article discusses the changes in system behavior that arise as parameter variations lead to the appearance of grazing intersections between quasiperiodic attractor and a two-dimensional impact surface in a three-dimensional state space. The occurrence of such "nonsmooth Hopf bifurcation" was briefly discussed in a book by Leine and Nijmeijer.[35] The purpose of the present article is to study the transition to quasiperiodicity through a border-collision bifurcation and to examine different examples of this process both numerically and experimentally. In one such example, an ergodic torus is born simultaneously with a period-5 saddle and a stable period-5 node. We have also observed that the stable cycle on the resonance torus can be born as a focus rather than as a node, like it is the case for smooth systems. Next, we consider the transitions between an ergodic torus and a resonant torus and show that the involved mechanisms are distinctly different from the mechanisms known for smooth systems. We also discuss how torus destruction can take place via a homoclinic bifurcation in the piecewise-linear model map. This analysis involves the use of numerical methods that can follow the stable and unstable manifolds for the various modes.

Finally, using a dc–dc buck converter with two-level control as an example, we experimentally verify the occurrence of torus birth bifurcations in piecewise-smooth dynamical systems.

II. THE PIECEWISE LINEAR NORMAL FORM

As we are interested in the dynamics near a border-crossing fixed point, the torus birth bifurcation can be investigated by using a piecewise-linear approximation to the piecewise-smooth map close to that point. It has previously been shown that this map, through a series of coordinate transformations, can be expressed on the normal form[19]

$$F:\begin{pmatrix} x \\ y \end{pmatrix} \mapsto \begin{cases} F_1(x,y), & x \le 0 \\ F_2(x,y), & x \ge 0, \end{cases} \tag{1}$$

where

$$F_1(x,y) = \begin{pmatrix} \tau_L x + y + \mu \\ -\delta_L x \end{pmatrix};$$

$$F_2(x,y) = \begin{pmatrix} \tau_R x + y + \mu \\ -\delta_R x \end{pmatrix}, \quad (x,y) \in \mathbb{R}^2.$$

In this representation the phase plane is divided into two halves, $L=\{(x,y):\ x\le 0,\ \ y\in\mathbb{R}\}$ and $R=\{(x,y):\ x>0,\ \ y\in\mathbb{R}\}$. τ_L and δ_L denote the trace and the determinant, respectively, of the Jacobian matrix J_L in the left-hand side half-plane, and τ_R and δ_R are the trace and determinant of the Jacobian matrix J_R in the right-hand side half. It is easy to show that

$$J_L = \begin{pmatrix} \tau_L & 1 \\ -\delta_L & 0 \end{pmatrix}, \quad J_R = \begin{pmatrix} \tau_R & 1 \\ -\delta_R & 0 \end{pmatrix}.$$

The theory of border-collision bifurcations developed so far assumes contractive dynamics at both sides of the discontinuity (i.e., $|\delta_L|<1$ and $|\delta_R|<1$).[23,25] By contrast, we consider a situation where an attracting fixed point changes into a spirally repelling fixed point as it moves across the border.

The stability of a fixed point is determined by the eigenvalues of the corresponding Jacobian matrix $\lambda_{1,2}=\frac{1}{2}(\tau\pm\sqrt{\tau^2-4\delta})$. Following di Bernardo *et al.*,[22] we indicate a stable fixed point in L by A and an unstable one by a. Similarly, stable and unstable fixed points in R will be denoted by B and b, respectively. These fixed points are determined by

$$A \text{ or } a = \left(\frac{\mu}{1-\tau_L+\delta_L}, \frac{-\mu\delta_L}{1-\tau_L+\delta_L} \right), \tag{2}$$

$$B \text{ or } b = \left(\frac{\mu}{1-\tau_R+\delta_R}, \frac{-\mu\delta_R}{1-\tau_R+\delta_R} \right). \tag{3}$$

For the fixed point A or a to actually exist, we must have $\mu/(1-\tau_L+\delta_L)\le 0$, otherwise a *virtual* fixed point is located in R and denoted as $\bar{A}$ or $\bar{a}$. Similarly, for B or b to actually occur, one needs $\mu/(1-\tau_R+\delta_R)\ge 0$. Otherwise a virtual fixed point is located in L, and denoted as $\bar{B}$ or $\bar{b}$.

As the parameter μ in map (1) is varied from a negative to a positive value, the fixed point moves from L to R, and

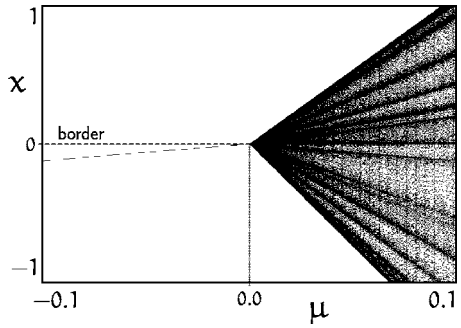

FIG. 1. Bifurcation diagram for the normal form map as the parameter μ varies from −0.1 to 0.1. The diagram shows a direct transition from a period-1 orbit to a quasiperiodic orbit. The other parameters are $\tau_L = 0.6765$, $\tau_R = 1.5$, $\delta_L = 0.5$, and $\delta_R = 1.6$.

the border collision, at which the fixed point crosses between the two regions, occurs at $\mu = 0$. Let us choose the parameters such that $\delta_L < 1$ and $\delta_R > 1$. The conditions

$$-(1+\delta_L) < \tau_L < 1+\delta_L, \quad -2\sqrt{\delta_R} < \tau_R < 2\sqrt{\delta_R} \tag{4}$$

then ensure that the fixed point is attracting for $\mu < 0$ and a spiral repeller for $\mu > 0$.

Let us now investigate the character of this transition. As the parameter μ crosses the bifurcation point at $\mu = 0$, a stable fixed point A on the L side turns into an unstable focus point b on the R side, and trajectories near the fixed point start to spiral outward. When the spiralling trajectory crosses back through the boundary to the L side, its dynamics will be guided by the attracting virtual fixed point $\bar{A}$ located in R. In this way the outward motion of the trajectory is arrested on the R side, and the system displays a rotating motion, controlled by the complex conjugated eigenvalues of b, but limited to a finite amplitude. This allows for the existence of an invariant closed curve on which the stationary state must lie. Figure 1 shows the bifurcation diagram with μ varied from a negative to a positive value. This diagram illustrates the abrupt transition from periodic to quasiperiodic behavior in a border-collision bifurcation. By contrast to the classic Neimark–Sacker bifurcation, the border-collision bifurcation is characterized by a linear growth in amplitude of the quasiperiodic dynamics as μ increases beyond the bifurcation point.

III. TRANSITIONS BETWEEN MODE-LOCKED DYNAMICS AND QUASIPERIODICITY

If one of the other parameters of map (1) is varied within the range delineated by (4), one can observe more complicated bifurcational transitions. To illustrate these phenomena, we have calculated the chart of dynamical modes (or two-parameter bifurcation diagram) in the parameter plane (τ_L, τ_R) for positive values of μ.

As shown in Fig. 2, this chart is characterized by a dense set of periodic tongues. Between the tongues there are parameter combinations that lead to quasiperiodicity. The bifurcation diagram in Fig. 3, calculated for $\tau_R = 5\tau_L/3$ (i.e., along the main diagonal of Fig. 2), shows the successively occurring regions of periodic and aperiodic behavior.

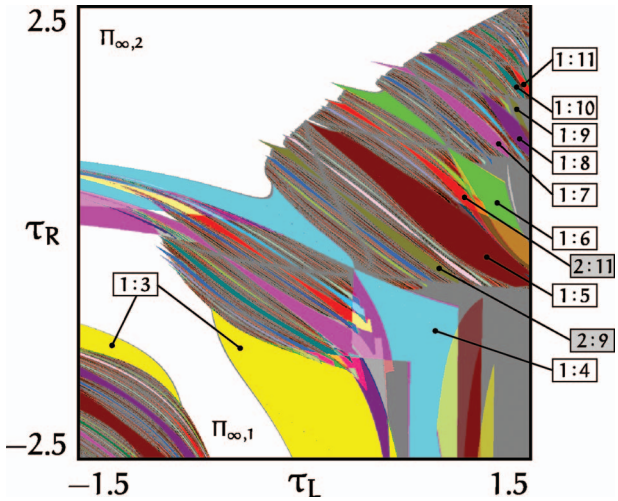

FIG. 2. (Color) Chart of dynamical modes of the normal form map in the parameter plane (τ_L, τ_R) with the remaining parameters fixed at $\delta_L = 0.5$, $\delta_R = 1.6$, and $\mu = 0.05$.

In the chart of dynamical modes shown in Fig. 2, $\Pi_{\infty,1}$ and $\Pi_{\infty,2}$ are domains where the trajectories of the map diverge to infinity for all initial conditions. Like for smooth systems, the tongues of periodicity can be ordered in accordance with the level of complexity.[44] Tongues of the first level of complexity have rotation numbers of the form $r:q = 1:m$, $m = 3,4,5\ldots$. Between any two tongues of the kth level of complexity, $k \geq 1$ with the rotation numbers r_k^m/q_k^m and r_k^{m+1}/q_k^{m+1} there are two infinite sequences of tongues of the $(k+1)$th level of complexity with the rotation numbers[44]

$$\frac{r_{k+1}^s}{q_{k+1}^s} = \frac{s r_k^m + r_k^{m+1}}{s q_k^m + q_k^{m+1}}, \quad \frac{r_{k+1}^s}{q_{k+1}^s} = \frac{r_k^m + s r_k^{m+1}}{q_k^m + s q_k^{m+1}}.$$

Here, $s = 1,2,\ldots$ is the number of the tongue in the sequence. The first sequence accumulates in the tongue with the rotation number r_k^m/q_k^m, and the second accumulates in the tongue with the rotation number r_k^{m+1}/q_k^{m+1}.

Low-periodicity tongues of the first level of complexity (and a few of the second level of complexity) are specified in the chart of dynamical modes (Fig. 2) by their respective rotation numbers. The level of complexity is indicated by the background color of the rotation number in the small tags: White corresponds to the first level of complexity and gray to the second.

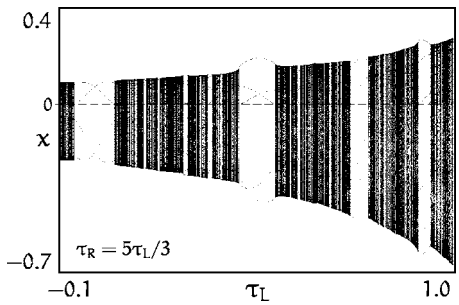

FIG. 3. Bifurcation diagram calculated for the section $\{(\tau_L, \tau_R): -0.1 \leq \tau_L \leq 1.0; \tau_R = 5\tau_L/3\}$ situated along the main diagonal of Fig. 2. The diagram shows repeated transitions between mode locking and quasiperiodicity.

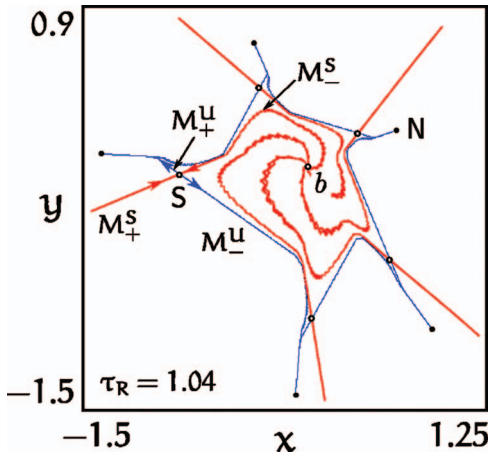

FIG. 4. (Color) Phase portrait of the normal form map within the 1:5 tongue of periodicity for $\tau_L=0.3$, $\delta_L=0.5$, $\tau_R=1.04$, $\delta_R=1.6$, and $\mu=0.05$. Here b is the fixed point, N and S are the node and saddle period-5 cycles, and $M^S_\pm$ and $M^U_\pm$ are the stable and unstable manifolds, respectively, of the saddle S.

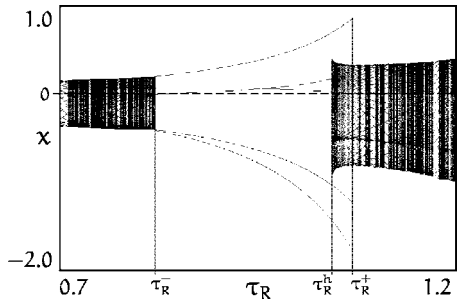

FIG. 5. Bifurcation diagram where τ_R is varied from 0.9 to 1.2 whereas the other parameters are fixed at $\tau_L=0.3$, $\delta_L=0.5$, $\delta_R=1.6$, and $\mu=0.05$. This diagram shows a hysteretic transition between mode locking and quasiperiodicity. τ_R^- and τ_R^+ are the border-collision fold bifurcation points. τ_R^h is the point of transition from quasiperiodic to periodic dynamics. The periodic orbit coexists with quasiperiodicity within the region $\tau_R^h < \tau_R < \tau_R^+$, where $\tau_R^h \approx 1.0425$ and $\tau_R^+ \approx 1.068\,785$.

In piecewise-linear systems the resonance tongues in parameter plane display a lens-like form (see Fig. 2). This structure was first described by Yang and Hao[45] for the case of a one-dimensional piecewise-linear map and was subsequently generalized to the case of higher-dimensional piecewise-smooth systems.[37,46] The latter work also presented a detailed bifurcation analysis of the resonance tongues and showed that the tongues are bounded by curves where stable and unstable cycles of different types merge and disappear in a border-collision bifurcation. We will refer to such a border-collision bifurcation as a *border-collision fold bifurcation* (an alternative denotation used in previous publications[5,23] is *border-collision pair bifurcation*).

With the exception of the 1:5 tongue, the tongues situated above the region of divergence $\Pi_{\infty,1}$ comprise more than one "lens" separated by so-called shrinking points where the width of the tongues reduces to zero.[45,47] At the shrinking points the boundaries of the tongue intersect. These points correspond to border-collision bifurcations where the periodic orbit continuously transforms from one type into another (i.e., border-collision bifurcations leading to a *simple change of the solution type*) as the parameter point passes from one lens to the next.

If $\mu<0$ then map (1) has a single nontrivial stable fixed point with a negative x coordinate. When μ changes sign, the x coordinate of the fixed point also changes sign and the fixed point abruptly loses stability: the stable focus transforms into an unstable focus. If the chosen parameter values correspond to a tongue of periodicity, then stable and saddle cycles softly arise from the fixed point. These cycles are located on a closed invariant curve composed of the unstable manifolds of the saddle and the points of two cycles. An example of such a curve is shown in Fig. 4 for the 1:5 tongue. The stable closed invariant curve of the resonance torus arises from the fixed point in a border-collision bifurcation.

Let us now study the bifurcational transitions from mode locking to quasiperiodicity. Figure 5 displays a bifurcation diagram illustrating the transition from the 1:5 mode-locking tongue to quasiperiodicity. The fifth iterate map, (1), has five stable fixed points and five saddle fixed points. If the parameter τ_R increases or decreases, the stable and unstable fixed points collide and disappear in a border-collision fold bifurcation at the points τ_R^+ and τ_R^-, respectively. Between the points $\tau_R^h \approx 1.0425$ and $\tau_R^+ \approx 1.068\,785$ the stable periodic orbit coexists with a quasiperiodic state. Figure 5 allows us to conclude that hard hysteretic transitions from one dynamical mode to another take place in the points τ_R^h and τ_R^+. For example, with increasing τ_R a hard transition from a periodic to a quasiperiodic orbit takes place at τ_R^+. Similarly, if the system follows the quasiperiodic oscillations with decreasing τ_R one observes the reverse transition to the periodic orbit at the point τ_R^h. It is interesting to note that precisely the same phenomenon is observed in our experiments with a power electronic dc–dc converter as described in Sec. IV.

Let us consider the characteristics of the bifurcational behavior shown in Fig. 5 in more detail in order to understand the mechanism of the transition between mode locking and quasiperiodicity. Within the mode-locking window there is a stable closed invariant curve (see Fig. 4). Our numerical analysis shows that, with increasing τ_R, the invariant curve loses its smoothness near the point τ_R^h.

In the initial state (Fig. 4), the system displays a closed invariant curve that is the union of the unstable manifold of the saddle cycle of period 5 and the points of the stable and saddle period-5 cycles. The closed invariant curve is piecewise smooth with sharp cusps in the node points. As the trace τ_R increases, in the point $\tau_R \approx 1.041\,812$, the manifolds become tangent to each other, and this leads to the formation of a nontransversal homoclinic orbit (see Fig. 6). With the further increase of τ_R, the stable and unstable manifolds of the period-5 saddle cycle intersect transversally to form the homoclinic structure.[48,49] The intersection of the two manifolds implies the existence of a Smale horseshoe and, as a consequence, of an infinite number of long-periodic orbits.[48] The stable and saddle five cycles continue to exist after the closed invariant curve has been destroyed. With further increase of τ_R, the stable and saddle cycles merge and disappear in a border-collision fold bifurcation.

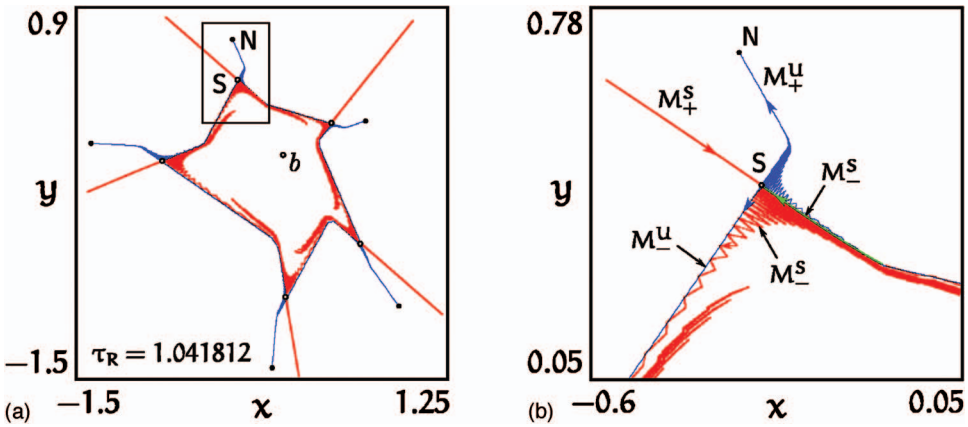

FIG. 6. (Color) (a) Homoclinic tangency appearing at $\tau_R \approx 1.041\,812$. (b) Magnified part of the phase portrait outlined by the rectangle in (a).

Figure 7 shows the phase portrait at $\tau_R=1.05$ after the closed invariant curve is destroyed. Here the stable period-5 node N coexists with the quasiperiodic orbit designated as C in Fig. 7(a). This quasiperiodic orbit arises after the second homoclinic tangency[48,49] at the point τ_R^h. Hence, there is a region where the stable cycle coexists with quasiperiodic dynamics. We have previously shown[50] that this region is bounded by the bifurcation curve of the second homoclinic tangency and by the curve of the border-collision fold bifurcation.

If we choose the parameters τ_L and τ_R in the region between the second homoclinic tangency and the border-collision fold bifurcation then a pair of stable and saddle period-5 cycles arise together with the quasiperiodic orbit as the fixed point crosses the borderline $x=0$. Figure 7(b) presents the bifurcation diagram for such transition, with μ as parameter.

We note how two coexisting stable orbits (periodic and quasiperiodic) appear as the period-1 orbit becomes unstable. Near the bifurcation point, when μ has a very small positive value, the radii of the basins of attraction of the coexisting orbits can be arbitrarily small. In this case the existence of even weak sources of noise, such as truncation errors in the computer simulations, can lead to a nonmonotonic behavior of the disturbance, and we can expect the appearance of nondeterminate dynamics. This represents a fundamental source of uncertainty[51,52] as to which attractor the system goes.

The tongues in the chart of dynamical modes (Fig. 2) intersect. This represents the occurrence of regions of multistability. For example, the 1:4 resonance tongue intersects with the 1:3 tongue of the first level of complexity and other tongues of the second and larger levels of complexity. When the closed invariant curve is destroyed, several stable periodic orbits coexist. Figures 8(a) and 8(b) show the phase portrait of the map for $\tau_L=0.35$ and $\tau_R=-1.157$, where the stable period-4 orbit coexists with the closed invariant curve. Figure 8(b) is a magnification of the region outlined by the rectangle in Fig. 8(a). The closed invariant curve is the union of the unstable manifold of the saddle cycle of period 7 and the points of the stable focus and saddle period-7 cycles. Figure 8(c) shows a phase portrait of the map for $\tau_L=1.384$ and $\tau_R=0.089$ after the closed invariant curve is destroyed. Here the stable period-5 orbit coexists with the stable period-6 cycle.

In the first case [illustrated by Figs. 8(a) and 8(b)], if we choose the parameters τ_L and τ_R in the region of multistability, varying μ from a negative to a positive value causes the stable closed invariant curve to arise together with one (or more) stable periodic orbits as the fixed point crosses the borderline $x=0$. In the other case [Fig. 8(c)], a bifurcational transition takes place where several coexisting stable period cycles arise from the fixed point in a border-collision bifurcation. It is interesting to note that these transitions can lead directly from a stable focus fixed point to a stable cycle of focus type lying on an attracting closed invariant curve.

IV. EXPERIMENTAL CONFIRMATION

In the present section, we consider a concrete example in the form of a multilevel pulse-width modulated dc-dc buck

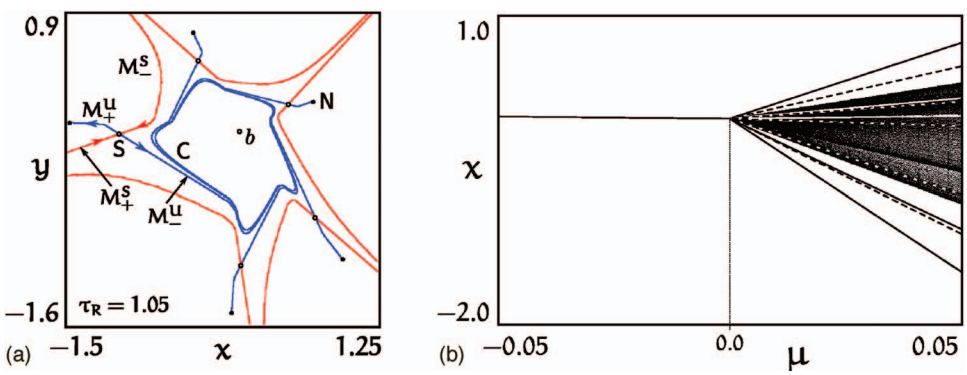

FIG. 7. (Color) (a) Phase portrait of the map after the closed invariant curve has been destroyed. Here the stable period-5 cycle N coexists with the quasiperiodic orbit C. The basins of attraction of the periodic and quasiperiodic orbits are separated by the stable manifold of the period-5 saddle cycle. (b) Bifurcation diagram illustrating the birth of a pair of stable and saddle period-5 cycle together with the quasiperiodic orbit from the fixed point through a border-collision bifurcation with varying μ. Other parameters are the same as in (a).

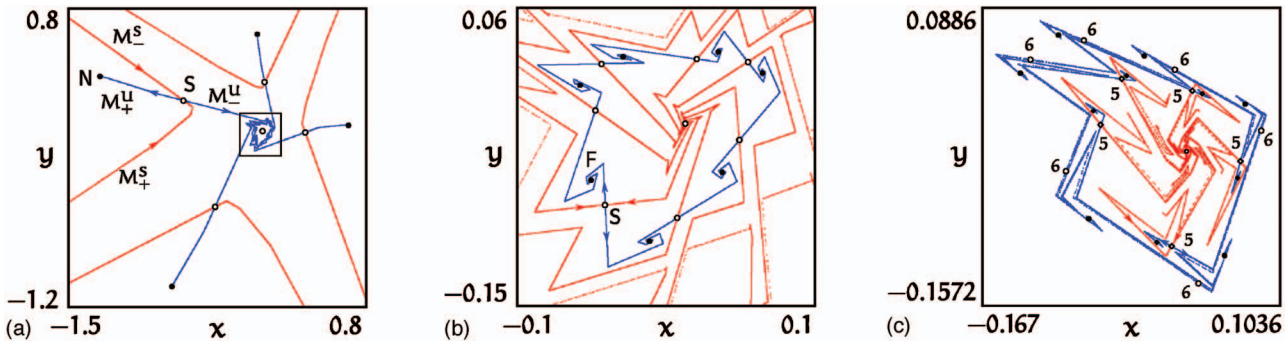

FIG. 8. (Color) Phase portraits of the map in the region of multistability. The small open circle in the middle represents the unstable fixed point. (a) Stable period-4 cycle coexisting with the closed invariant curve. (b) Magnified part of the phase portrait outlined by the rectangle in (a). The closed invariant curve is the union of the unstable manifold of the saddle cycle of period 7 and the points of the stable focus F and saddle S period-7 cycles. (c) Phase portrait of the map for the case when the closed invariant curve does not exist. Stable period-5 cycle coexists here with a stable period-6 cycle. The numbers 5 and 6 mark period-5 and period-6 saddle points, respectively.

converter,[53–58] and experimentally confirm that the phenomena observed for the piecewise linear normal form map (1) actually occur in practical systems. More concretely, we present the first experimental observation of the transition from periodicity to quasiperiodicity through a border-collision bifurcation.

Figure 9 shows a schematic diagram of the considered dc-dc power converter with two-level pulse-width modulation. The switches S_1 and S_2 may be realized, for instance, by metal-oxide-semiconductor field-effect transistors that can operate with more than 50 000 switchings per second. To understand the way of working of this converter, let us first suppose that comparator 2 and switch S_2 are excluded from the circuit. In this case we have a simple dc-dc buck converter with single-zone regulation as described, for instance, by Aroudi *et al.*[42] As switch S_1 opens and closes, the voltage applied to the *LC* filter varies between input voltage and zero. The *LC* filter smooths the signal to be applied to the load resistor *R* into a relatively constant voltage of a value lower than that of the input voltage. It is usually desirable to regulate the output voltage to a prescribed value. This can be achieved by controlling the switching process through a feedback mechanism. A simple method, called voltage-mode control, implies that a voltage proportional to the output voltage v_C is compared with a reference voltage V_{ref} to generate a control voltage v_{con}. This control voltage is compared with a sawtooth waveform V_{ramp} to generate the switching signal. The switch is turned on at the beginning of every ramp period, and is turned off when the ramp voltage exceeds the value of the control voltage at the beginning of the ramp cycle (this is sometimes called pulse-width modulation of type 1). The output voltage approaches $E_0/2$ when S_1 is closed, and v_C tends to 0 when S_1 is open. The electronic circuit itself is linear, and the nonlinearities arise from the switching processes that alter the structure and, hence, the dynamics of the system.

The system we consider in this article is a variant of the previous scheme which is applicable when two or more input

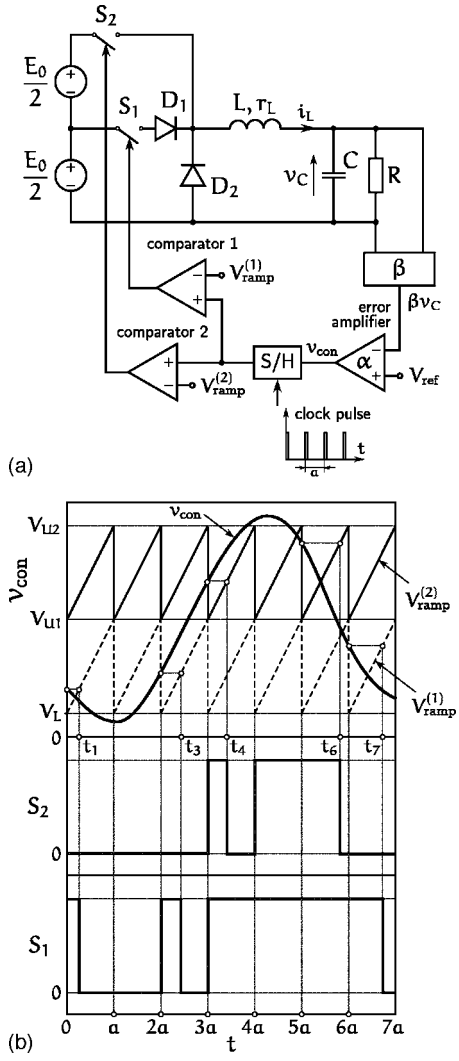

FIG. 9. (a) Schematic diagram of the dc–dc buck converter with two-level control. Here S/H is the sample–hold unit. (b) Generation of switching signals *S*1 and *S*2 in a two-level controlled buck converter. *a* denotes the period of the ramp function.

voltage levels are available, or easily obtainable from a single voltage source. The scheme is implemented by using two ramp signals– $V_{\text{ramp}}^{(1)}$ between V_L and V_{U1}, and $V_{\text{ramp}}^{(2)}$ between V_{U1} and V_{U2}, both driven by the same clock. As illustrated in Fig. 9, the control voltage is given by

$$v_{\text{con}} = \psi(X) = \alpha(V_{\text{ref}} - \beta v_C).$$

α and β are referred to as the amplification constant for the corrector and the transfer parameter for the voltage sensor, respectively. If the value of v_{con} at the beginning of a ramp cycle falls between V_L and $V_{U1}=V_L+U_0/2$ (zone 1), the control signal generates a closing signal to switch S_1 as long as it exceeds $V_{\text{ramp}}^{(1)}$. If v_{con} at the beginning of a ramp cycle lies between V_{U1} and $V_{U2}=V_L+U_0$ (zone 2), it is compared with $V_{\text{ramp}}^{(2)}$ to generate a closing signal to switch S_2. The generation of these switching signals for a typical control voltage waveform is illustrated in Fig. 9(b).

Period T of a periodic mode is an integer multiple of the period of the ramp signal, i.e., $T=ma$, where $m=1,2,\ldots$ Such an operation of the converter will be referred to as a period-m mode, or m cycle. It is clear from Fig. 9(b) that when the converter operates in a period-1 mode, only one pulse-width modulated signal can be generated. Two types of period-1 cycles are possible for a system with two-level modulation. The first type corresponds to the case where the value of the control voltage v_{con} at the beginning of a ramp cycle lies in zone 1 and the control pulse is produced only by comparator 1. In this case, switch S_2 remains open. The second type corresponds to the case where the control voltage lies in zone 2 and the control pulse is produced by comparator 2 [see Fig. 9(a)]. In this case switch S_1 remains closed.

In our earlier work[50] we have performed a detailed bifurcation analysis of a converter of this type. We have shown that the dynamics of this converter can be described by means of a stroboscopic map that is piecewise smooth.[50] We had obtained the chart of dynamical modes for this map and showed how torus birth can take place either via a classical Neimark–Sacker bifurcation or via a border-collision bifurcation.

The period-1 cycle changes its type through a border collision bifurcation when, with the change of a parameter, the value of the control voltage at a clock instant coincides with V_{U1}, i.e., the boundary between the two levels. At such an event, depending on the parameter values, we may observe a variety of different scenarios. The first possibility is the continuous transformation of the stable period-1 cycle into a stable period-1 cycle of another type. This transition involves an abrupt change in the multipliers of the cycle. However, none of the multipliers leave the unit circle, and the system does not undergo a bifurcation.

A second possibility is that a stable focus is transformed into an unstable focus and that a quasiperiodic orbit arises from the fixed point in a border-collision bifurcation. This bifurcation is characterized by the abrupt jump of the fixed point's complex conjugate eigenvalues from the inside to the outside of the unit circle. Moreover, the amplitude of the produced quasiperiodic oscillations varies linearly with the distance from the bifurcation point (see Fig. 1).

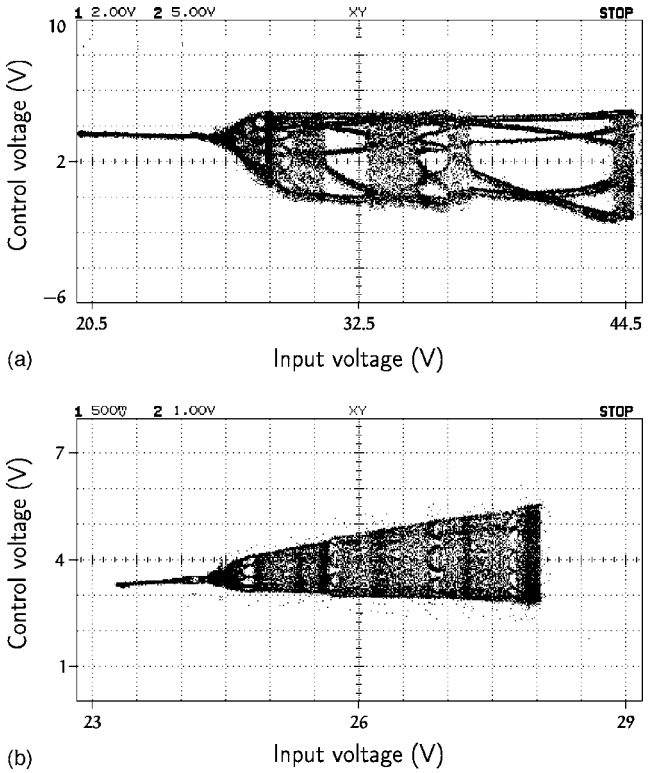

FIG. 10. (a) Experimental bifurcation diagram of the two-level controlled buck converter with the input voltage as a bifurcation parameter and (b) close-up of the parameter region where the transition to quasiperiodicity takes place.

We have implemented the previous control scheme in a two-zone dc-dc converter with the following parameters: $R=126\ \Omega$, $L=0.11$ H, $r_L=13.5\ \Omega$, $C=1\ \mu$F, $V_{\text{ref}}=2.5$ V, $V_L=0.6$ V, $V_{U1}=3.1$ V, $V_{U2}=5.5$ V, $\beta=0.22$, $\alpha=10$, $T=150\ \mu$s. Here, L and C denote the inductance and the capacitance, respectively, of the LC filter, R is the load resistance, and r_L is a parasitic resistance characterizing the dissipation in the inductance coil.

The input voltage E_0 is used as a bifurcation parameter. The experimentally obtained bifurcation diagram is shown in Fig. 10. The diagram shows a transition from periodicity to quasiperiodicity at $E_0 \approx 24.5$ V, and, as the parameter is further increased, we observe a series of periodic windows with mode-locked behavior.

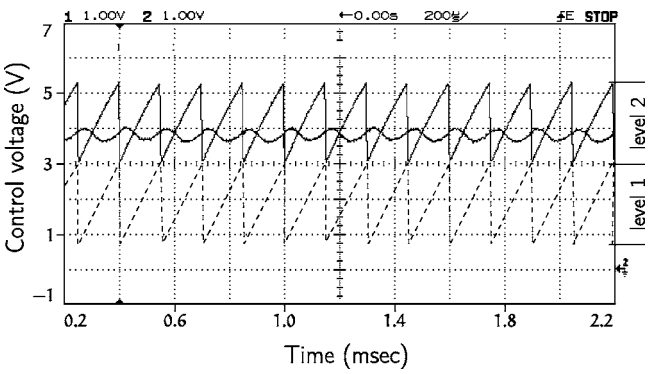

FIG. 11. Experimental waveforms of the converter under regular periodic operation at $E_0 \approx 20.3$ V.

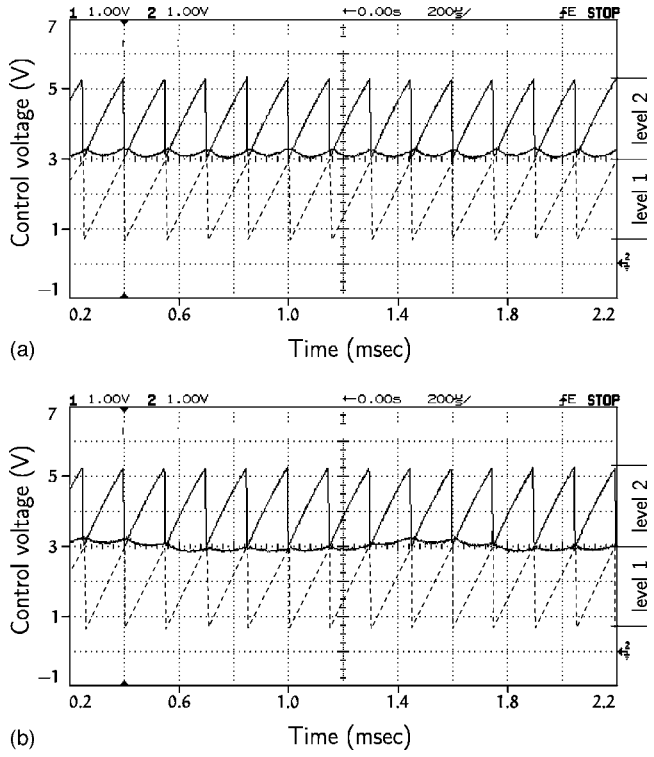

FIG. 12. (a) Waveforms just before the transition to quasiperiodicity at $E_0 \approx 23.6$ V and (b) just after the transition, $E_0 \approx 24.8$ V. Note how the strictly periodic dynamics in (a) becomes modulated by a slower dynamics in (b).

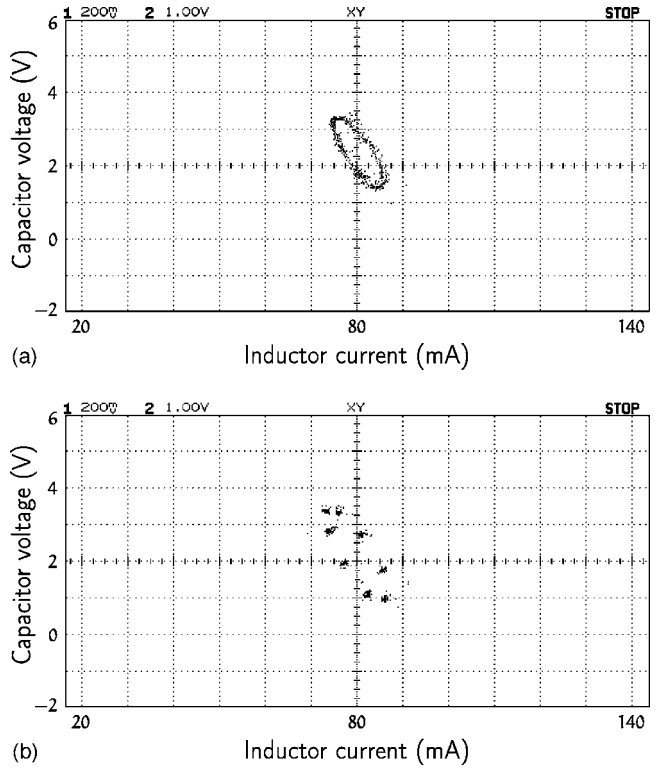

FIG. 13. Phase portraits on the Poincaré section, (a) for the quasiperiodic dynamics at $E_0 \approx 31.9$ V and (b) for the 1:8 mode-locked dynamics for $E_0 \approx 32.9$ V. Note how the closed invariant curve for the ergodic torus turns into a set of discrete points for the resonance torus.

Figure 11 shows the waveforms of the control voltage and the ramp voltages under normal periodic operation. At every clock instant, the control voltage is in zone 2. As the input voltage is increased, v_{con} approaches the boundary between the two zones and, when the control voltage hits the border, the behavior abruptly changes into quasiperiodicity. This is illustrated in Fig. 12, and we conclude that the transition is caused by a border-collision bifurcation.

Immediately following this bifurcation, the amplitude of the lower frequency component is small [as seen in Fig. 12(b)]. However, the amplitude increases with increasing bifurcation parameter and, as the input voltage is increased to $E_0 \approx 32$ V, we observe the emergence of a periodic window. Figure 13 shows the discrete-time phase portraits as the states are observed in synchronism with the falling edge of the triangular waves. The phase portrait shows a closed invariant curve when the waveform is quasiperiodic. After the transition to periodicity, the dynamics produces a finite number of points placed on the invariant curve. In continuous time, this implies a transition from an ergodic torus to a resonance torus.

In order to explore the transition mechanism between quasiperiodicity and mode locking, Figs. 14(a) and 14(b) display the waveforms just before and after the transition from quasiperiodic to periodic orbit occurring at $E_0 \approx 32$ V. Detailed inspection of these waveforms seems to show that the transition is not caused by a border-collision bifurcation. Figures 14(c) and 14(d) show the waveforms just before and after the transition from periodic to quasiperiodic orbit as it occurs for $E_0 \approx 34$ V. In this transition the control voltage hits the boundary between the two regions, indicating that the transition is a border-collision event, presumably related to the border-collision fold bifurcation leading to the destruction of the periodic orbit. As discussed in Secs. III and IV, such a bifurcation is generally preceded by a homoclinic bifurcation, and there is a parameter range where the periodic and quasiperiodic orbits coexist.

On the curves of border-collision fold bifurcation and homoclinic tangency one can expect hysteretic transitions from periodic to quasiperiodic orbit or vice versa (see Figs. 5 and 7). Such transitions are also observed experimentally. The bifurcation diagrams obtained by varying the input voltage in opposite directions (Fig. 15) show hysteresis at the right-hand side of the period-5 window. This confirms our theoretical predictions. Figure 15(a) illustrates the transition from quasiperiodic orbit to period-5 cycle with decreasing input voltage E_0, and Fig. 15(b) illustrates the transition from period-5 cycle to quasiperiodic orbit with increasing E_0. The bifurcation points in the two diagrams are marked by the dashed lines. The bifurcations are seen to occur somewhat below and somewhat above $E_0 = 42$ V, respectively.

V. CONCLUSION

The appearance of quasiperiodic dynamics has repeatedly been observed in recent numerical studies of various piecewise-smooth systems,[35,37,39,40,42,43,46] and it has been reported that such behavior can appear through a smooth Neimark–Sacker bifurcation as well as through a border collision bifurcation.

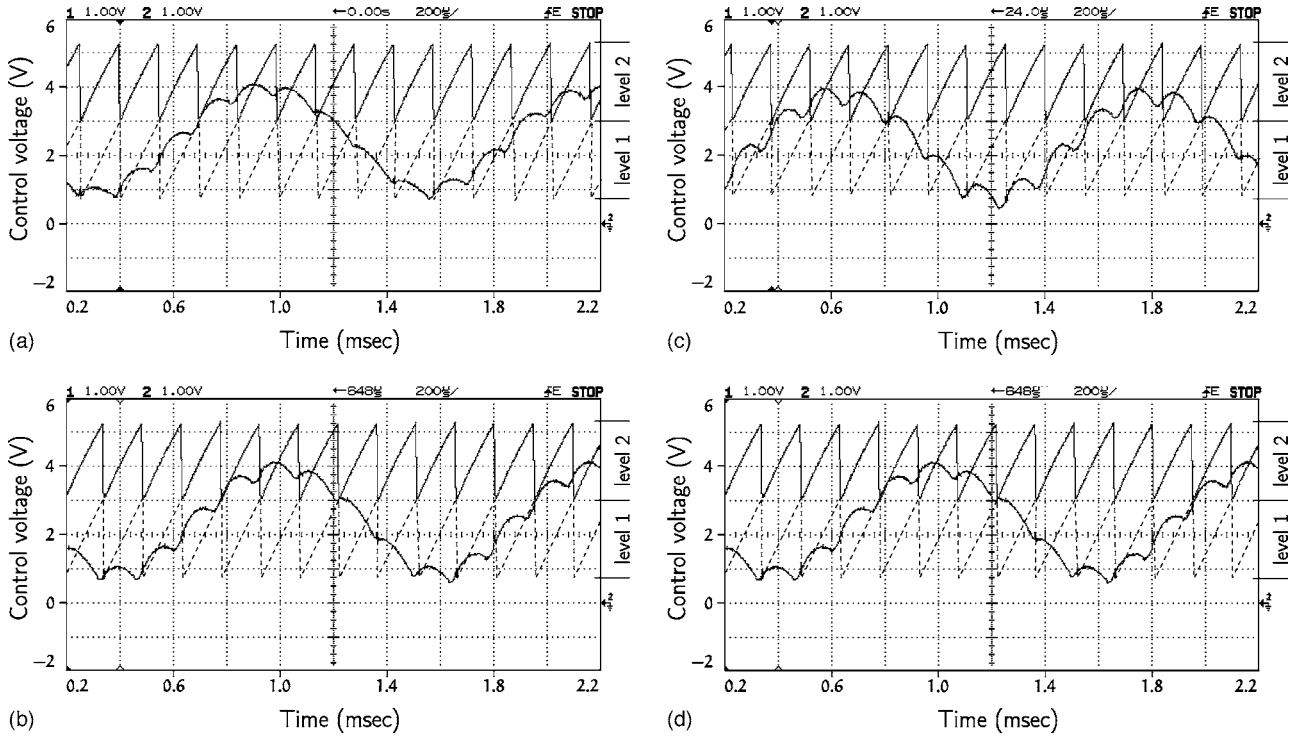

FIG. 14. The waveforms (a) before the transition from ergodic torus to resonance torus, $E_0 \approx 31.9$ V, (b) after the transition, $E_0 \approx 32.3$ V, (c) before the transition from resonance torus to ergodic torus, $E_0 \approx 33.5$ V, and (d) after the transition, $E_0 \approx 34.7$ V.

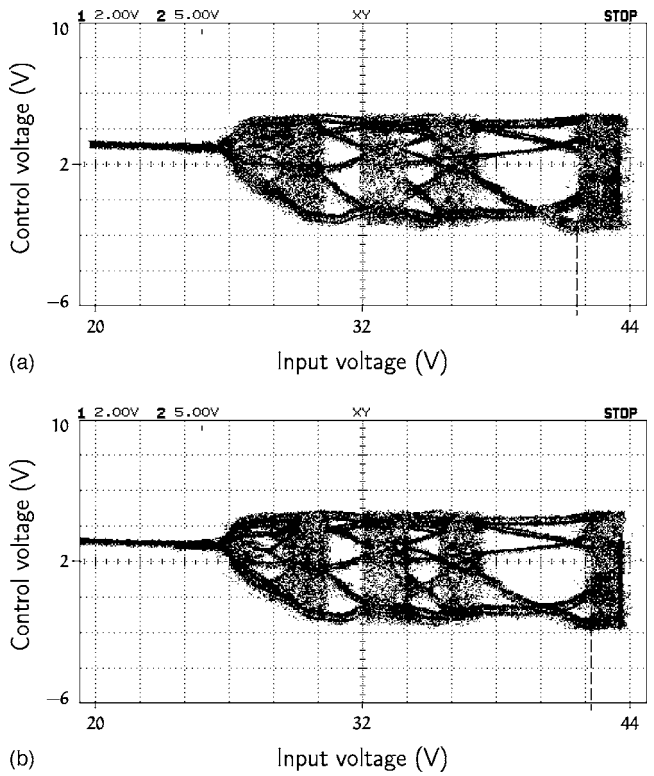

FIG. 15. Experimental bifurcation diagram illustrating the hysteretic transition from periodic to quasiperiodic orbit and vice versa (indicated by the punctuated lines): (a) when the input voltage decreases and (b) when the input voltage increases.

Border-collision bifurcations are distinguished from the local bifurcations we know for smooth systems by the fact that the eigenvalues of the considered modes can make abrupt jumps in the complex plane. Representing the analogue of the classical Neimark–Sacker bifurcation (Hopf bifurcation for maps) in which a pair of complex conjugate eigenvalues under variation of a parameter continuously move out of the unit circle, the birth of quasiperiodicity through border collision bifurcation is marked by an abrupt jump of a complex conjugate pair of eigenvalues from the inside of the unit circle to the outside.

Based on the normal form map that represents the behavior of the system in a close neighborhood of the border, we have investigated the transition from a stable fixed point (regular cycle in the continuous-time system) to a stable closed invariant curve associated with periodic or quasiperiodic dynamics via a border-collision bifurcation.

The chart of dynamical modes for the normal form map was obtained through a detailed numerical study. This chart is characterized by a dense set of resonance zones. The transitions between mode-locked dynamics and quasiperiodicity are shown to occur in the following way. Inside of each tongue with the rotation number r:q there is a closed invariant curve that is the union of the unstable manifold of the period-q saddle and the points of the stable (node or focus) and saddle period-q cycles. When the parameters are changed, this closed invariant curve may be destroyed through a homoclinic bifurcation. However, the stable and saddle cycles continue to exist after the destruction of the

closed invariant curve to finally disappear at the boundaries of the tongue through a border-collision fold bifurcation. Therefore, in the parameter plane between the lines of homoclinic bifurcation and border-collision fold bifurcation there is a multistability region. On the boundaries of this region one can observe hysteretic transitions. This multistability was illustrated by two examples in which the stable period-5 cycle coexisted, respectively, with quasiperiodic dynamics and with a stable period-6 cycle. In both cases detailed phase plots were presented showing, besides the various steady states, also the associated invariant manifolds.

Using a dc–dc converter with multilevel pulse-width modulation as an example, we have also experimentally shown that the phenomena observed for the piecewise linear normal form map actually occur in practical systems. The verified phenomena include the occurrence of

(i) a border-collision torus birth bifurcation when the input voltage exceeds a certain threshold value;
(ii) border-collision fold bifurcations in connection with the transitions from periodic to quasiperiodic attractor; and
(iii) hysteresis (associated with a homoclinic bifurcation and a border-collision fold bifurcation) in the transition between mode locking and quasiperiodicity.

To our knowledge, these are the first experimental verifications of torus-related border collision bifurcations in piecewise-smooth dynamical systems.

ACKNOWLEDGMENTS

This work was supported in part by the Department of Atomic Energy, The Government of India under Project No. 2003/37/11/BRNS and in part by Danish Natural Science Foundation through the Center for Modelling, Nonlinear Dynamics and Irreversible Thermodynamics (MIDIT). Figures 4, 6, 7(a), and 8 were generated with DsTool.[59–61]

[1] I. Gumowski and C. Mira, *Recurrence and Discrete Dynamic Systems*, Lecture Notes in Mathematics Vol. 809 (Springer, Berlin, 1980).
[2] J. H. B. Deane and D. C. Hamill, IEEE Trans. Power Electron. **5**, 260 (1990).
[3] M. Ohnishi and N. Inaba, IEEE Trans. Circuits Syst., I: Fundam. Theory Appl. **41**, 433 (1994).
[4] E. Fossas and G. Olivar, IEEE Trans. Circuits Syst., I: Fundam. Theory Appl. **43**, 13 (1996).
[5] G. H. Yuan, S. Banerjee, E. Ott, and J. A. Yorke, IEEE Trans. Circuits Syst., I: Fundam. Theory Appl. **45**, 707 (1998).
[6] T. Kousaka, T. Ueta, and H. Kawakami, IEEE Trans. Circuits Syst., II: Analog Digital Signal Process. **46**, 878 (1999).
[7] E. Toribio, A. El Aroudi, G. Olivar, and L. Benadero, IEEE Trans. Power Electron. **15**, 1163 (2000).
[8] B. Brogliato, *Nonsmooth Mechanics—Models, Dynamics and Control* (Springer, New York, 1999).
[9] A. B. Nordmark, J. Sound Vib. **145**, 279 (1991).
[10] C. Budd and F. Dux, Philos. Trans. R. Soc. London **347**, 365 (1994).
[11] B. Thuilot, A. Goswami, and B. Espiau, "Bifurcation and chaos in a simple passive bipedal gait," *IEEE International Conference Robotics Automation*, Albuquerque, NM, 1997.
[12] M. Garcia, A. Chatterjee, A. Ruina, and M. Coleman, J. Biomech. Eng. **120**, 281 (1998).
[13] J. Keener and J. Sneyd, *Mathematical Physiology* (Springer, New York, 1998).
[14] O. Sosnovtseva and E. Mosekilde, Int. J. Bifurcation Chaos Appl. Sci. Eng. **7**, 1225 (1997).
[15] M. I. Feigin, Prikl. Mat. Mekh. **34**, 861 (1970) (in Russian).
[16] M. I. Feigin, Prikl. Mat. Mekh. **38**, 810 (1974) (in Russian).
[17] M. I. Feigin, Prikl. Mat. Mekh. **42**, 820 (1978) (in Russian).
[18] M. I. Feigin, *Forced Oscillations in Systems with Discontinuous Nonlinearities* (Nauka, Moscow, 1994) (in Russian).
[19] H. E. Nusse and J. A. Yorke, Physica D **57**, 39 (1992).
[20] H. E. Nusse, E. Ott, and J. A. Yorke, Phys. Rev. E **49**, 1073 (1994).
[21] H. E. Nusse and J. A. Yorke, Int. J. Bifurcation Chaos Appl. Sci. Eng. **5**, 189 (1995).
[22] M. di Bernardo, M. I. Feigin, S. J. Hogan, and M. E. Homer, Chaos, Solitons Fractals **10**, 1881 (1999).
[23] S. Banerjee and C. Grebogi, Phys. Rev. E **59**, 4052 (1999).
[24] S. Banerjee, M. S. Karthik, G. H. Yuan, and J. A. Yorke, IEEE Trans. Circuits Syst., I: Fundam. Theory Appl. **47**, 389 (2000).
[25] S. Banerjee, P. Ranjan, and C. Grebogi, IEEE Trans. Circuits Syst., I: Fundam. Theory Appl. **47**, 633 (2000).
[26] M. Di Bernardo, C. Budd, and A. Champneys, Nonlinearity **11**, 859 (1998).
[27] M. di Bernardo, C. J. Budd, and A. R. Champneys, Phys. Rev. Lett. **86**, 2553 (2001).
[28] M. di Bernardo, C. J. Budd, and A. R. Champneys, Physica D **160**, 222 (2001).
[29] M. di Bernardo, P. Kowalczyk, and A. Nordmark, Physica D **170**, 175 (2002).
[30] M. di Bernardo, P. Kowalczyk, and A. Nordmark, Int. J. Bifurcation Chaos Appl. Sci. Eng. **13**, 2935 (2003).
[31] A. B. Nordmark, Nonlinearity **14**, 1517 (2001).
[32] P. T. Piironen, L. N. Virgin, and A. R. Champneys, J. Nonlinear Sci. **14**, 383 (2004).
[33] *Nonlinear Phenomena in Power Electronics: Attractors, Bifurcations, Chaos, and Nonlinear Control*, edited by S. Banerjee and G. C. Verghese (IEEE Press, Piscataway, NJ, 2001).
[34] B. Blazejczyk-Okolewska, K. Czolczynski, T. Kapitaniak, and J. Wojewoda, *Chaotic Mechanics in Systems with Impacts and Friction* (World Scientific, Singapore, 1999).
[35] R. I. Leine and H. Nijmeijer, *Dynamics and Bifurcations of Non-Smooth Mechanical Systems* (Springer, Berlin, 2004).
[36] C. K. Tse, *Complex Behavior of Switching Power Converters* (CRC Press, Boca Raton, FL, 2003).
[37] Z. T. Zhusubaliyev and E. Mosekilde, *Bifurcations and Chaos in Piecewise-Smooth Dynamical Systems* (World Scientific, Singapore, 2003).
[38] M. di Bernardo, F. Garofalo, L. Glielmo, and F. Vasca, "Quasi-periodic behaviors in DC–DC converters," in *IEEE Power Electronic Special Conference* (IEEE, Piscataway, NJ, 1996), pp. 1376–1381.
[39] A. El Aroudi, L. Benadero, E. Toribio and S. Machiche, Int. J. Bifurcation Chaos Appl. Sci. Eng. **10**, 359 (2000).
[40] A. E. Aroudi and R. Leyva, IEEE Trans. Circuits Syst., I: Fundam. Theory Appl. **48**, 967 (2001).
[41] Z. T. Zhusubaliyev, E. A. Soukhoterin, and E. Mosekilde, IEEE Trans. Circuits Syst., I: Fundam. Theory Appl. **50**, 1047 (2003).
[42] A. El Aroudi, M. Debbat, R. Giral, G. Olivar, L. Benadero, and E. Toribio, Int. J. Bifurcation Chaos Appl. Sci. Eng. **15**, 1549 (2005).
[43] H. Dankowicz, P. Piiroinen, and A. B. Nordmark, Chaos, Solitons Fractals **14**, 241 (2002).
[44] Yu. L. Maistrenko, V. L. Maistrenko, S. I. Vikul, and L. O. Chua, Int. J. Bifurcation Chaos Appl. Sci. Eng. **5**, 653 (1995).
[45] W. M. Yang and B. L. Hao, Commun. Theor. Phys. **8**, 1 (1987).
[46] Z. T. Zhusubaliyev, E. A. Soukhoterin, and E. Mosekilde, Chaos, Solitons Fractals **13**, 1889 (2002).
[47] I. Sushko, L. Gardini, and T. Puu, Chaos, Solitons Fractals **21**, 403 (2004).
[48] Yu. A. Kuznetsov, *Elements of Applied Bifurcation Theory*, 3rd ed. (Springer, New York, 2004).
[49] A. Agliari, G.-I. Bischi, R. Dieci, and L. Gardini, Int. J. Bifurcation Chaos Appl. Sci. Eng. **15**, 1285 (2005).
[50] Z. T. Zhusubaliyev and E. Mosekilde, Phys. Lett. A **351**, 167 (2006).
[51] T. Kapitaniak and Yu. L. Maistrenko, Phys. Rev. E **58**, 5161 (1998).
[52] M. Dutta, H. E. Nusse, E. Ott, J. A. Yorke, and G.-H. Yuan, Phys. Rev. Lett. **83**, 4281 (1999).
[53] A. V. Kobzev, *Multilevel Pulse Modulation: Theory and Applications to Power Electronics* (Nauka, Novosibirsk, 1979).
[54] P. M. Bhagwat and V. R. Stefanovic, IEEE Trans. Ind. Appl. **IA-19**, 1057 (1983).

[55]A. V. Kobzev, G. Ya. Mikhal'chenko, and N. M. Muzhitchenko, *Modulating Power Supplies of Radioelectronic Devices* (Radio i Svyaz, Tomsk, 1990).
[56]G. Carrara, S. Gardella, M. Marchesoni, R. Salutari, and G. Sciutto, IEEE Trans. Power Electron. **7**, 497 (1992).
[57]J. S. Lai and F. Z. Peng, IEEE Trans. Ind. Appl. **32**, 509 (1996).
[58]F. Z. Peng, IEEE Trans. Ind. Appl. **37**, 611 (2001).
[59]A. Back, J. Guckenheimer, M. R. Myers, F. J. Wicklin, and P. A. Worfolk, Not. Am. Math. Soc. **39**, 303 (1992).
[60]B. Krauskopf and H. M. Osinga, in *Numerical Methods for Bifurcation Problems and Large-Scale Dynamical Systems*, edited by E. J. Doedel and L. S. Tuckerman (Springer, New York, 2000), pp. 199–208.
[61]J. P. England, B. Krauskopf, and H. M. Osinga, SIAM J. Appl. Dyn. Syst. **3**, 161 (2004).